Journal of Catalysis **203,** 25–32 (2001)
doi:10.1006/jcat.2001.3315, available online at http://www.idealibrary.com on IDEAL®

Reactive Oxygen Species in Titanosilicates TS-1 and TiMCM-41: An *In Situ* EPR Spectroscopic Study

K. Chaudhari, D. Srinivas, and P. Ratnasamy[1]

National Chemical Laboratory, Pune 411 008, India

Received October 30, 2000; revised June 13, 2001; accepted June 13, 2001; published online August 28, 2001

The superoxide species generated by the interaction of titanosilicate molecular sieves, TS-1 and TiMCM-41, with aqueous H_2O_2 have been studied by EPR spectroscopy. Three paramagnetic Ti(IV)-superoxide radical species (A, B, and C, respectively) have been observed in TS-1 samples; mainly species B has been identified in TiMCM-41. The Ti(IV) ions in the superoxide are in framework positions. Species B is more abundant than species A and C. On interaction with aqueous H_2O_2 the geometry of titanium expands from tetra- to hexacoordination in species A and C and to pentacoordination in species B. The EPR spectra of the Ti(IV)-superoxide species are characterized by rhombic *g* tensors. The effects of solvents, substrate (allyl alcohol), and temperature on the EPR spectra and distribution of species A–C have been examined. *In situ* **EPR studies have revealed that species A and C are more reactive toward the oxidation of allylalcohol to the corresponding epoxide than species B. Variable-temperature EPR studies (77–190 K) have provided evidence, for the first time, of the superoxide–hydroperoxide/peroxide interconversions. At higher temperatures Ti(IV)-superoxide is the preferred geometry. At lower temperatures Ti(IV)-hydroperoxide/peroxide is formed. Species B did not exhibit such an interconversion. It is concluded that, in addition to the framework Ti centers being able to expand their coordination geometry from 4 to 6 and the hydrophobic nature of the titanosilicate structure, the relative concentrations of the superoxide and hydroperoxide/peroxide under reaction conditions are crucial factors determining catalytic activity and, especially, selectivity.**

Key Words: **titanosilicates; TS-1; TiMCM-41; microporous materials; mesoporous materials; Ti(IV)-superoxide; Ti(IV)-hydroperoxide; Ti(IV)-peroxide; EPR; structure; oxidation of allyl alcohol; oxidation with H_2O_2; structure–activity correlation.**

INTRODUCTION

Titanosilicates, particularly TS-1, have been widely studied due to their remarkable catalytic properties in the selective oxidation of organic compounds with hydrogen peroxide under mild conditions (1, 2). Several factors including the method of preparation, crystallite size, impurities (such as alkali ions, Al(III), TiO_2 particles, etc.), and solvent affect the catalytic activity of TS-1 catalysts (3–12). EPR spectroscopy is a powerful technique to investigate the *local structure* of the catalytically active species such as the oxo-titanium radical ions. Studies using EPR spectroscopy of titanosilicates are limited due to the +4 oxidation state and consequent diamagnetic nature of titanium. Indirect evidence for the tetrahedral geometry of Ti in TS-1 and TiMCM-41 samples was, however, obtained by reducing the samples (with CO or H_2 or by irradiation with γ rays) to EPR-active Ti(III) species (13–16). One of the intriguing features of catalysis by titanosilicates is that although titanium has a tetrahedral geometry in both TS-1 and TiMCM-41, their catalytic activities in the presence of H_2O_2 are different. TS-1 exhibits high activity and selectivity while TiMCM-41 does not (17–21). Perhaps, an understanding of the structure, concentration, and role of the oxo-titanium species that are formed on these two titanosilicates under reaction conditions may explain such differences.

Three oxygenated Ti species (Ti(IV)-peroxide, -hydroperoxide, and -superoxide), shown in Fig. 1, have been claimed to be active in oxidations over titanosilicates (1, 2, 10, 22, 23). We had reported, earlier, on the catalytic oxidations of allyl and methallyl alcohols, allyl and methallyl chlorides, acrolein, and methacrolein using aqueous H_2O_2 as the oxidant and TS-1 as the catalyst (23). A Ti(IV)-hydroperoxide species was thought to be responsible for the oxidation of the alcohol to aldehyde while epoxidation originated from a Ti(IV)-superoxide species (23). An interesting observation was that for a given TS-1 sample, the product distribution (selectivity) was dependent also on the nature of the solvent used (23).

In the present study, we investigate the structure of the oxo-titanium species in TS-1 and TiMCM-41, using *in situ* and variable-temperature EPR spectroscopy. The oxo-titanium species were formed by interaction with 30% aqueous H_2O_2. The effect of solvents on the structure of the oxo-titanium species has also been investigated. The Ti contents of the samples (Si/Ti = 36 in TS-1 and 46 in TiMCM-41) were chosen such that most, if not all, of the titanium ions are present as isolated titanium species and

[1] To whom correspondence should be addressed. E-mail: prs @ems.ncl.res.in. Fax: (91)-20-5893355.

0021-9517/01 $35.00

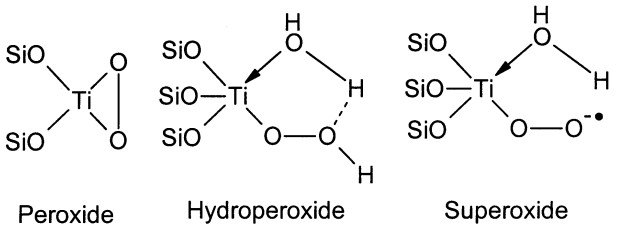

FIG. 1. Reactive oxygen species in titanosilicates.

occupy only the framework substitutional positions. A detailed EPR study of the oxo-titanium species formed over TS-1 and TiMCM-41 on interaction with H_2O_2 has, so far, not been published.

EXPERIMENTAL

Materials

Aqueous tetrapropylammonium hydroxide (20%, aq. TPAOH solution), tetraethylorthosilicate (TEOS), and titanium tetrabutoxide [$Ti(OBu)_4$] obtained from Aldrich Co. were used in the preparation of TS-1 samples. Fumed silica (99%, Sigma), tetramethylammonium silicate (TMA silicate; 10 wt% silica solution, $TMA/SiO_2 = 0.5$; SACHEM Inc.), cetyltrimethylammonium chloride/hydroxide (CTMACl/OH; 17.9 wt% Cl and 6.7 wt% OH) prepared in the laboratory by partial exchange of CTMACl (25 wt% aqueous solution, Aldrich) over an ion exchange resin, tetramethylammonium hydroxide (TMAOH; 99%, Aldrich), and Ti butoxide (Aldrich) were used in the preparation of TiMCM-41.

Sample Preparation

TS-1. Titanosilicate TS-1 was synthesized according to the published procedure of Thangaraj *et al.* (24, 25).

TiMCM-41. In the synthesis of TiMCM-41, the molar composition of the synthesis gel in terms of oxides was as follows:

$$SiO_2 : 0.02TiO_2 : 0.089(CTMA)_2O : 0.155(TMA)_2O : 18H_2O.$$

In a typical synthesis, 24.6% solution of CTMACl/OH (16.7 g) was taken in a polypropylene beaker and 2.08 g TMAOH dissolved in 10 g water and 13.6 g TMA silicate were added to it while stirring. The thick gel formed was stirred for 15 min. Fumed silica (3.1 g) was then added slowly in about 10 min to the above mixture under stirring. The stirring was continued for 1 h after complete addition. To this thick slurry, 0.52 g of $Ti(OBu)_4$ in 5–6 g of isopropanol was added. Stirring was continued for 1 h. The pH of the final slurry was maintained at 11.5. The mixture was then transferred to a stainless steel autoclave and heated at 383 K for 5 days. The solid material (TiMCM-41) was filtered, washed with deionized water, and dried at 373 K in air. The product was then calcined at 823 K, first, in flowing nitrogen (for 3 h) and, then, in flowing air (for 6 h) to remove the organic matter.

Sample Characterization

The X-ray diffractograms of calcined titanosilicalite samples were recorded on a Rigaku Miniflex diffractometer using nickel filtered CuKα radiation ($\lambda = 1.5406$ Å, 30 kV, 15 mA) over $2\theta = 5^\circ$–50° and scan speed $= 4^\circ$/min for TS-1 and over $2\theta = 1.5^\circ$–10° and scan speed $= 1^\circ$/min for TiMCM-41. The chemical composition was estimated using a Rigaku 3070 E wavelength dispersive XRF spectrometer with a Rh target energized at 50 kV and 40 mA. For XRF measurements glass beads of standards (TiO_2/SiO_2) and samples were prepared by the borate fusion technique. The surface area and pore diameter of the samples were determined from N_2 adsorption isotherms (obtained on a Coulter 100 instrument), using the Barret–Joyner–Halenda (BJH) model (26). The diffuse reflectance UV-visible (DRUV-vis) spectra of solid catalysts were recorded using a Shimadzu UV-2101 PC spectrometer. Fourier transform infrared (FT-IR) spectra of the samples as KBr pellets were recorded on a Pye Unicam SP-300 spectrophotometer. EPR spectra were measured using a Bruker EMX spectrometer operating at X-band frequency and 100-kHz field modulation. The samples were taken in Suprasil quartz tubes of outside diameter 4.5 mm. The spectra at 77 K were measured using a quartz finger dewar. Variable-temperature experiments (80–348 K) were done using a Bruker BVT 3000 temperature controller. Spectral simulations were performed using the Bruker Simfonia software package. The spectral intensities were measured from the double integration plots of the deconvoluted spectra.

Prior to EPR experiments the samples of TS-1 and TiMCM-41 were activated at 373 K under static air. Desired solvent (0.4 ml) was added to a known amount of activated solid catalyst (45 mg) such that the solid catalyst was completely soaked in the solvent. To this 0.1 ml of 30% aqueous H_2O_2 was added. Soon after the addition of H_2O_2 the color of the solid changed from white to yellow. In some experiments allyl alcohol (AA) was added prior to the addition of H_2O_2. In those cases the reaction was vigorous and exothermic. In the latter experiments the samples were heated at 333 K for 2 min and quenched immediately to 77 K to record the EPR spectra.

RESULTS

Physicochemical Characteristics of TS-1 and TiMCM-41

The crystallinity and phase purity of calcined TS-1 and TiMCM-41 samples were confirmed from their XRD

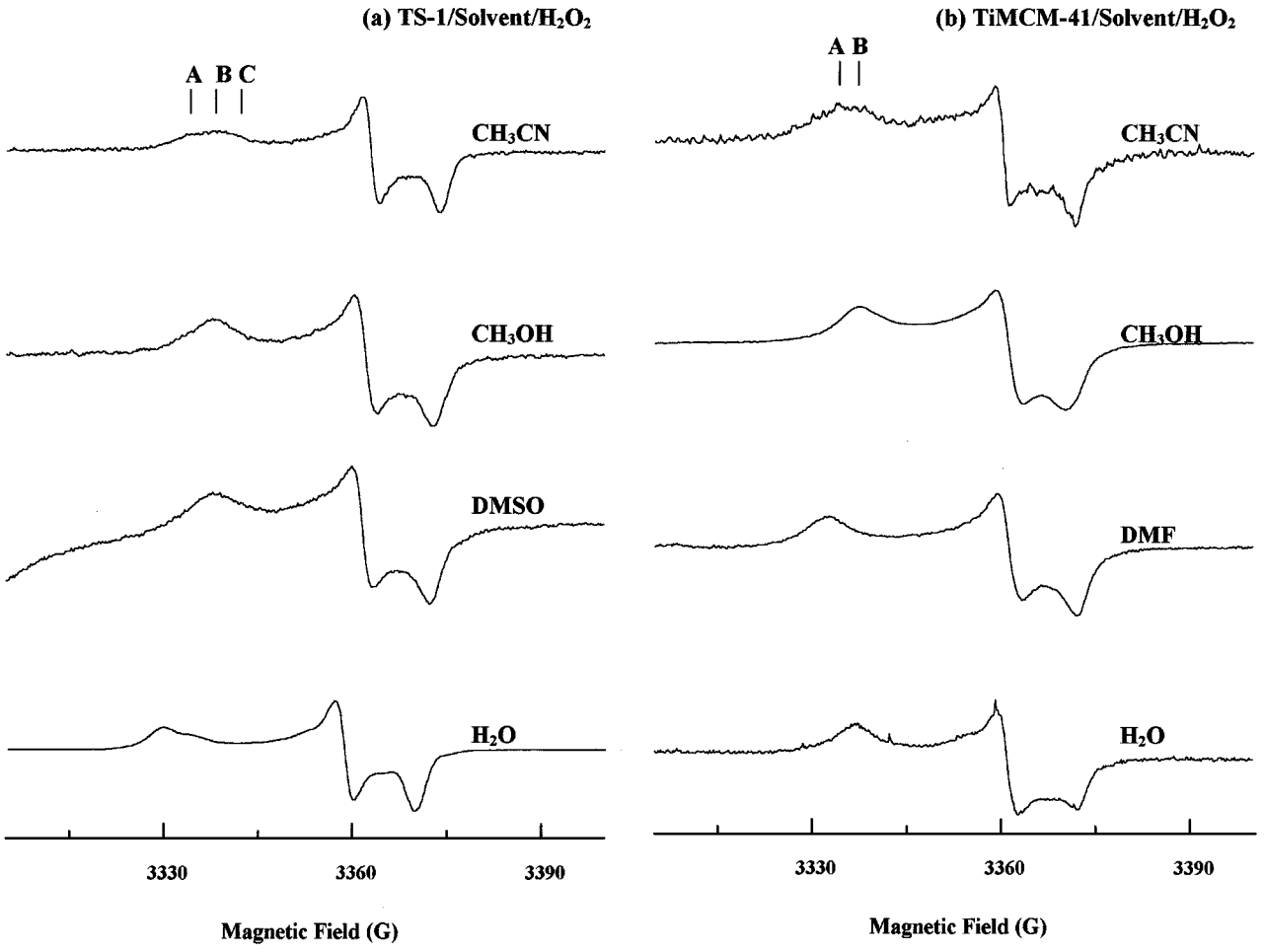

FIG. 2. X-band EPR spectra (77 K) of the interaction of H_2O_2 (30% aqueous) with (a) TS-1 and (b) TiMCM-1 in different solvents.

patterns (5, 17, 19, 21). TS-1 and TiMCM-41 exhibited band maxima at 208 and 224 nm, respectively, indicating the presence of isolated Ti(IV) centers in the silicate framework. The DRUV-vis spectra did not reveal the presence of any extra-framework anatase TiO_2 phase (27). FT-IR spectra showed the characteristic band at 968 cm^{-1} for TS-1 and 964 cm^{-1} for TiMCM-41 (28). The Si/Ti ratios (XRF) were 36 and 46 for TS-1 and TiMCM-41, respectively. The BET surface areas of the samples, from N_2 adsorption isotherms, were 400 and 963 m^2/g, for TS-1 and TiMCM-41, respectively. The pore volume of TiMCM-41 was 0.9 cm^3 and the average pore diameter was 30 Å.

Interaction of TS-1 and TiMCM-41 with Aqueous H_2O_2

Effect of solvent. Both TS-1 and TiMCM-41 showed no EPR signal revealing a +4 oxidation state of Ti in the silicate structures. On contact with 30% aqueous H_2O_2, the solid catalysts became yellow and exhibited three EPR signals, characteristic of a rhombic g tensor, at 77 K. Representative EPR spectra, recorded at 77 K, of TS-1 and TiMCM-41, in different solvents, after contact with aqueous H_2O_2 are shown in Figs. 2a and 2b, respectively. These spectra are typical of a Ti(IV)-superoxide radical species $Ti(O_2^{\bullet -})$ (29, 30).

Spectral simulations revealed three types of Ti(IV)-superoxide radical species (A, B, and C, respectively; Table 1) in TS-1. By contrast, mainly species B could be identified over TiMCM-41. In the presence of CH_3CN, however, both A and B were seen (Table 1). Species A, B, and C differ mainly in the values of their g_z parameter. The effect of solvent is pronounced, especially on the g_z value (Table 1). In strong donor solvents (such as DMF and DMSO), the g_z value (of species B of TiMCM-41) changes from 2.024 to 2.026, characteristic of species A, indicating the conversion of species B to A. This increase in the g_z parameter of TiMCM-41 in strong donor solvents probably arises from the coordination of the solvent molecules to the titanium site. Figure 3 shows the experimental, simulated, and deconvoluted spectra of the oxidized TS-1 samples in CH_3CN. Among the several possible combinations, the sets of g values presented in Table 1 yielded simulated spectra that closely resembled the experimental spectra.

TABLE 1

EPR Parameters of the Oxo-titanium(IV) Species

		TS-1					TiMCM-41				
Solvent	Species	g_z	g_y	g_x	Intensity ($\times 10^7$ a.u.)	Superoxide ($\times 10^{-5}$ mol)	g_z	g_y	g_x	Intensity ($\times 10^7$ a.u.)	Superoxide ($\times 10^{-5}$ mol)
CH_3CN	A	2.0264	2.0090	2.0023	2.757		2.0265	2.0093	2.0027	52.78	
	B	2.0235	2.0090	2.0023	2.763	3.8	2.0240	2.0093	2.0027	79.81	70.0
	C	2.0220	2.0090	2.0023	1.493		a	a	a	a	
CH_3CN/AA	B	2.0235	2.0090	2.0023	4.118	2.2	2.0243	2.0093	2.0027	6.245	3.3
$CH_2CH_2Cl_2$	B	2.0245	2.0095	2.0025	3.385	1.8	2.0245	2.0093	2.0026	4.767	2.6
$(CH_3)_2CO$	A	2.0265	2.0087	2.0018	0.787		a	a	a	a	
	B	2.0235	2.0087	2.0018	4.331	3.2	2.0245	2.0093	2.0026	9.521	5.1
	C	2.0210	2.0087	2.0018	0.831		a	a	a	a	
$(CH_3)_2CO$/AA	B	2.0235	2.0091	2.0023	2.404	1.3	2.0245	2.0093	2.0024	13.24	7.1
CH_3OH	A	2.0260	2.0090	2.0023	2.788		a	a	a	a	
	B	2.0235	2.0090	2.0023	7.039	6.2	2.0233	2.0090	2.0026	9.521	5.1
	C	2.0220	2.0090	2.0023	1.697		a	a	a	a	
CH_3OH/AA	B	2.0235	2.0090	2.0023	1.879	1.0	2.0242	2.0093	2.0027	5.233	5.8
CH_3CH_2OH/AA	B	2.0230	2.0093	2.0025	2.799	1.5	2.0242	2.0093	2.0025	14.15	7.6
DMF	A						2.0267	2.0090	2.0028	7.113	3.8
DMSO	A	2.0265	2.0093	2.0025	1.534		2.0258	2.0092	2.0028	8.816	4.7
	B	2.0240	2.0093	2.0025	7.176	5.4	a	a	a	a	
	C	2.0210	2.0093	2.0025	1.347		a	a	a	a	
H_2O	A	2.0266	2.0090	2.0023	153.7		a	a	a	a	
	B	2.0238	2.0090	2.0023	26.01	96.0	2.0240	2.0093	2.0027	26.61	14.2

Note. AA = allylalcohol; a = absent.

Effect of Temperature. Figure 4 shows the variation of $I(T)/I(180)$ with temperature for TS-1 and TiMCM-41. Here, $I(T)$ is the intensity of the g_y or g_z signal at temperature T and $I(180)$ is the intensity at 180 K. The overall spectral intensity of the Ti(IV)-superoxide species is more in TiMCM-41 than in TS-1 samples.

Oxidation of Allyl Alcohol over TS-1 and TiMCM-41 Catalysts—In Situ EPR Study

We have reported earlier that the oxidation of AA over TS-1 and VS-1 catalysts with aqueous H_2O_2 yields the corresponding epoxide, aldehyde, and acid products (23). Their relative concentrations depend critically on the solvent used. In $(CH_3)_2CO$ and CH_3CN (weakly polar solvents) the conversion and selectivity for epoxide were quite high over TS-1 catalysts. However, polar solvents such as CH_3OH and C_2H_5OH lowered both the conversion and epoxide selectivity. Over VS-1, however, aldehydes and acids were the major products (23). To gain a better understanding of the mechanistic aspects of this oxidation reaction, *in situ* EPR studies were conducted in 4.5-mm outer diameter quartz EPR sample tubes. Activated catalysts (45 mg) were initially treated with solvent (0.4 ml) and subsequently with the substrate, AA. To this mixture, aqueous H_2O_2 (0.1 ml) was added and the reaction mixture was heated at 350 K for 2 min. The reaction was exothermic, instantaneous, and vigorous. The samples were quenched immediately to 77 K and their EPR spectra were recorded. Typical spectra for TS-1 and TiMCM-41 in CH_3CN are shown in Fig. 5. It was interesting to note that the intensities of the signals due to species A and C were reduced in the presence of allyl alcohol; only species B was predominant. No noticeable changes in the g parameters of species B were observed in the presence of AA. A reduction in the overall spectral intensity was, however, observed as a function of time. These observations suggest that the oxo-titanium species A and C, being more reactive than B in their reaction with the substrate, are consumed faster.

Stability of the Ti(IV)-Superoxide at High Temperatures

Figures 6a and 6b show the interaction of H_2O_2 with TS-1 and TiMCM-41, respectively, in the range 298–348 K. Compared to the spectra at lower temperatures (see Fig. 2), the signals are narrower and well resolved. The better resolution and narrow signals at higher temperatures is, perhaps, due to, the enhanced rotation of the O–O bond (of Ti–O–O) around the Ti–O axis and the consequent shorter relaxation times. Both species A and B could be identified in the spectra of TS-1 samples (Fig. 6a); species C was absent. Only species B was present over TiMCM-41. As expected, the overall spectral intensity decreased at high temperatures. The relative stability of the three oxo-titanium species varied in the order B > A > C.

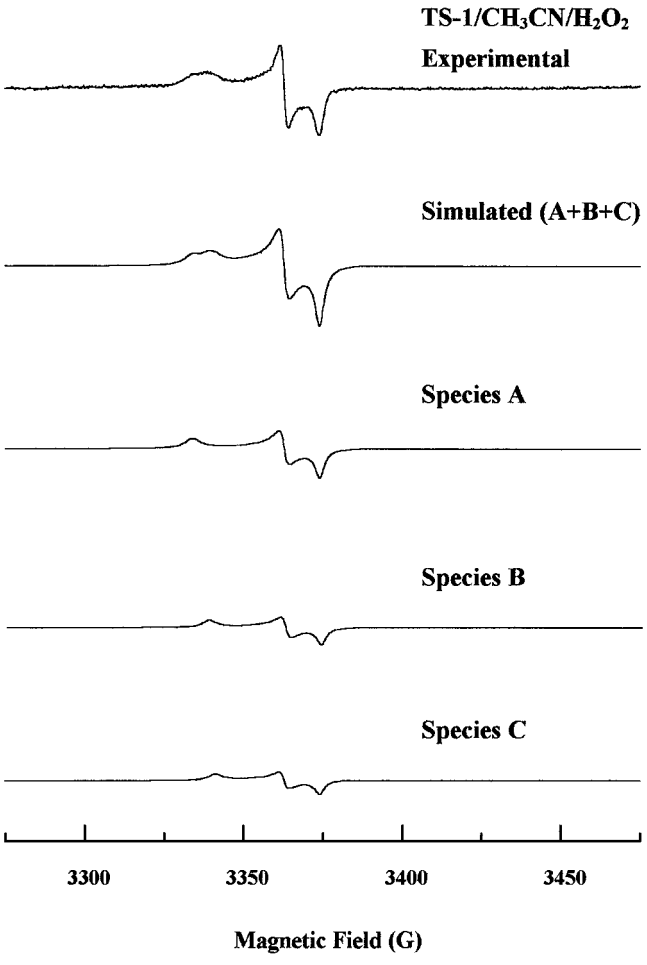

FIG. 3. Experimental, simulated, and deconvoluted (of species A, B, and C) EPR spectra (77 K) of TS-1–H_2O_2 interaction in the presence of CH_3CN.

DISCUSSION

The physicochemical characterization studies (XRD, surface area measurements, XRF, DRUV-vis, FT-IR, and EPR) have confirmed the phase purity, framework substitution, and +4 oxidation state of Ti in TS-1 and TiMCM-41 samples. Isolated Ti centers activate H_2O_2 and yield Ti(IV)-superoxide and Ti(IV)-hydroperoxide/peroxide species (Fig. 1). The former are paramagnetic while the latter are diamagnetic and EPR-inactive. EPR studies reveal three types of Ti(IV)-superoxide radicals: A, B, and C in TS-1 and mainly one (B or A) over TiMCM-41. The Ti(IV)-superoxide radicals have a rhombic symmetry consistent with a bent Ti–$O_2^{\bullet-}$ geometry. A, B, and C differ mainly in their g_z parameter. The spectrum of TiMCM-41 is more intense than that of TS-1. The free $O_2^{\bullet-}$ ion has an electronic configuration of $(1\sigma_g)^2(1\sigma_u)^2(2\sigma_g)^2(2\sigma_u)^2(3\sigma_g)^2(1\pi_u)^4(1\pi_g)^3$ with a $^2\Pi$ ground state. Interaction with the Ti centers removes the degeneracy of the HOMO π_g into π_g^x and π_g^y orbitals with energy separation Δ. The g-value expressions

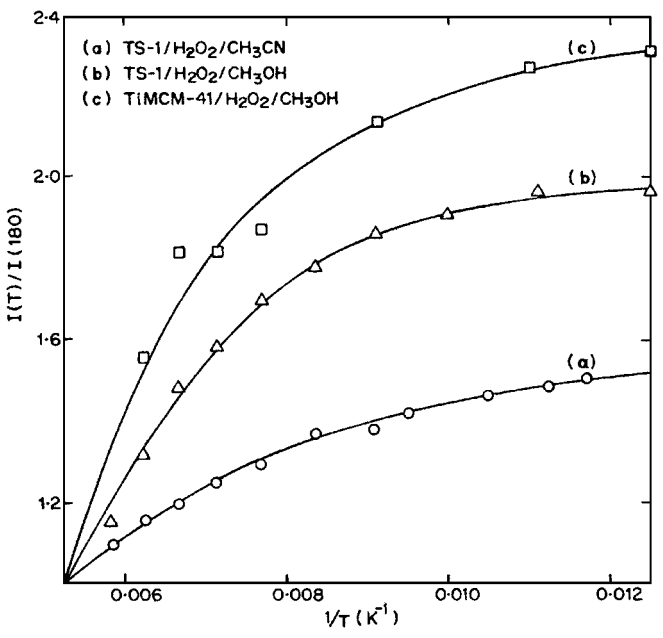

FIG. 4. Relative intensity variation ($I(T)/T(180)$) of the Ti(IV)-superoxide species as a function of temperature T. (a) TS-1/CH_3CN/H_2O_2; (b) TS-1/CH_3OH/H_2O_2; (c) TiMCM-41/CH_3OH/H_2O_2.

for $O_2^{\bullet-}$ radicals when $\lambda < \Delta \ll E$ and neglecting second-order terms can be written as (31, 32)

$$g_x \approx g_e,$$
$$g_y = g_e + 2\lambda/E, \qquad [1]$$
$$g_z = g_e + 2\lambda/\Delta,$$

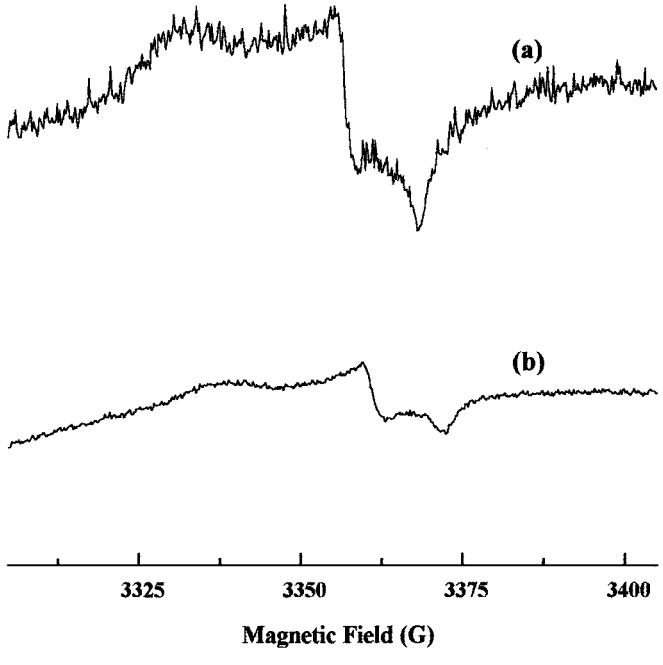

FIG. 5. EPR spectra at 77 K of (a) TiMCM-41/CH_3CN/allyl-alcohol/H_2O_2 and (b) TS-1/CH_3CN/allylalcohol/H_2O_2.

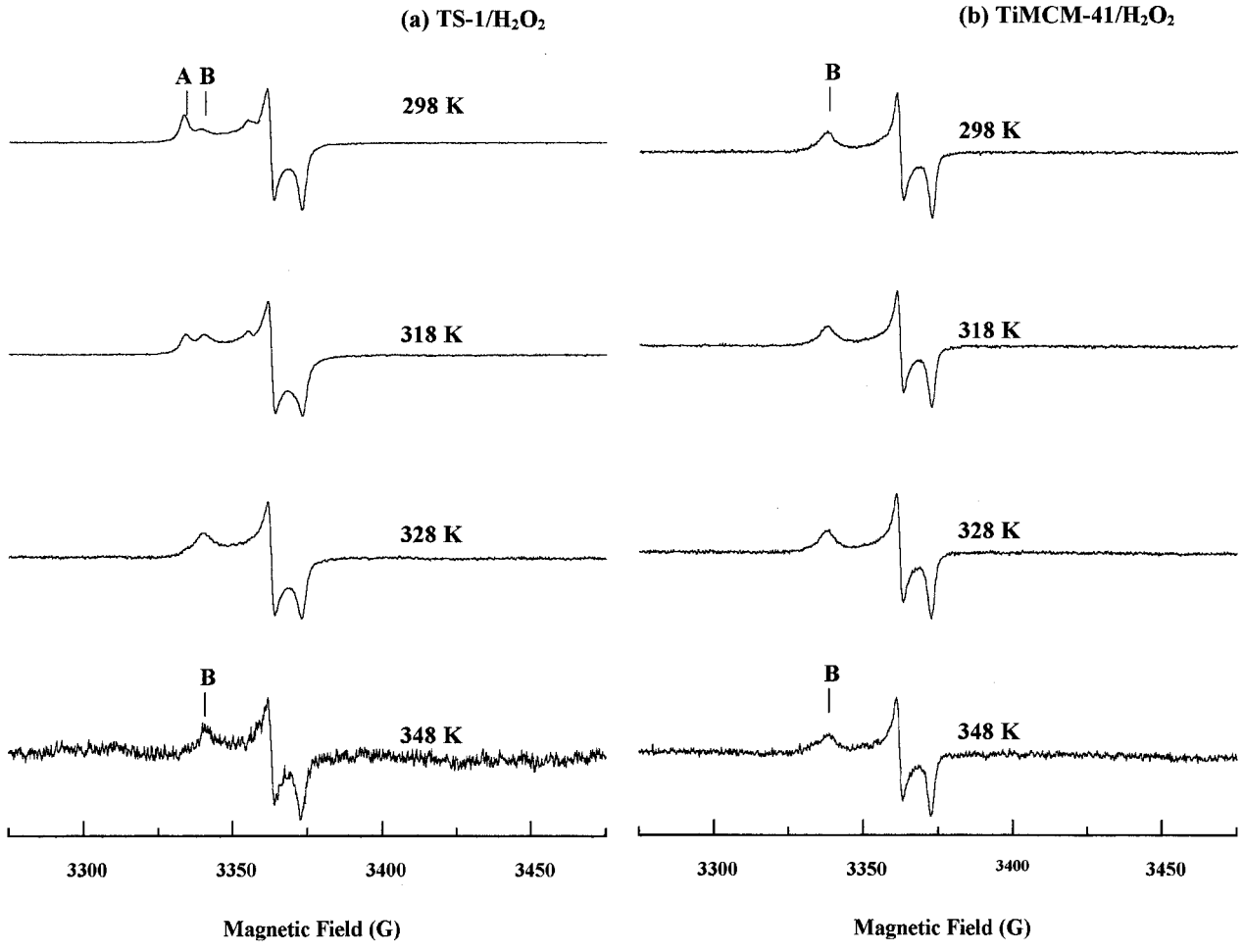

FIG. 6. Influence of temperature on the EPR spectra of the Ti(IV)-superoxide species (A and B) in (a) TS-1/H_2O/H_2O_2 and (b) TiMCM-41/H_2O/H_2O_2.

where g_e is the free-electron g value of 2.0023, λ is the spin orbit coupling constant (λ value for oxygen is 135 cm^{-1}), and E is the energy separation between $3\sigma_g$ and $1\pi_g^x$ orbitals. The g_z value of the superoxide radical anion is sensitive to the nature of the cation to which it is coordinated (Ti, in our case), its oxidation state, and the local coordination geometry (29, 30). By substituting the g_z values (from the spectra) in Eq. [1] the magnitude of Δ was estimated to be 11203, 12735, and 13705 cm^{-1} for species A, B, and C, respectively. Both the coordination number, and the Ti(IV)–$O_2^{\bullet-}$ ion distance influence the g_z value of the superoxide. The value of g_z decreases with a decrease in the Ti–$O_2^{\bullet-}$ bond distance. A comparison of the Ti($O_2^{\bullet-}$) values in anatase TiO_2 (31) as well as of ETS-4/–10 structures (16) suggests that the oxo-Ti(IV) ions in A and C possess sixfold coordination while pentacoordination occurs in species B (Fig. 7).

In order to probe the structural features of the Ti(IV)-$O_2^{\bullet-}$ radicals deeper, a known amount of $Ti(OBu)_4$ dissolved in isopropanol was contacted with aqueous H_2O_2. The color of the solution instantaneously changed to yellow. The solution exhibited an EPR spectrum typical of species B ($g_z = 2.0242$, $g_y = 2.0088$, and $g_x = 2.0023$). The spectral intensity of this sample was used as a reference to estimate the relative concentration of the Ti($O_2^{\bullet-}$) species

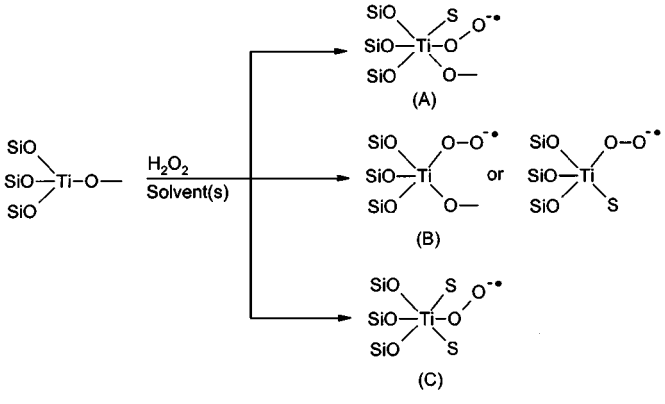

FIG. 7. Tentative structures of Ti(IV) species before and after the interactions with H_2O_2.

in both TS-1 and TiMCM-41 samples. The concentration of superoxide species estimated from the overall spectral intensity (Table 1) varies with the solvent and the silicate structure. On interaction with H_2O_2 the geometry of $Ti(OBu)_4$ changes from tetrahedral to pentacoordination. The similarity in g values of the superoxide radicals generated in the $Ti(OBu)_4$–H_2O_2 system and species B of TS-1 and TiMCM-41, hence, suggests a pentacoordinated geometry for titanium in species B.

The EPR parameters of species A are similar to those of the H_2O_2–TiO_2 on a porous Vycor glass system ($g_z = 2.0268$, $g_y = 2.0088$, and $g_x = 2.0036$) (27, 30, 33). The parameters of species C are similar to those of H_2O_2–ETS-4 and ETS-10 systems ($g_z = 2.021$, $g_y = 2.008$, and $g_x = 2.002$) (16). We therefore conclude from the spectral resemblance that Ti(IV) ions in species A and C possessing a tetrahedral geometry *before* the interaction with H_2O_2 expand their geometry to sixfold coordination *after* the interaction (Fig. 7). Similarly, the spectral resemblance of oxidized $Ti(OBu)_4$ and species B of both TS-1 and TiMCM-41 suggests that the Ti sites of species B expand their coordination geometry from tetrahedral to pentacoordination *after* the interaction (Fig. 7). The prominent effect of solvent on the g_z parameter of species B of TiMCM-41 suggests that the Ti sites in TiMCM-41 are accessible to solvent molecules. This observation is not surprising in view of the larger pore diameter of TiMCM-41. In highly coordinating solvents such as DMF and DMSO, species B in TiMCM-41 converts into species A. In contrast, in TS-1, species B could be identified even in DMSO-exposed samples. This suggests that at least part of species B in TS-1 are in locations which are not easily accessible to solvent molecules. From neutron diffraction studies Hijar *et al.* (34) recently concluded that in TS-1, titanium is distributed among only 4 or 5 of the 12 silicon sites. Sites such as T10, for example, will be less accessible for solvent molecules (see Fig. 6 of Ref. 34). In species A and C, the titanium geometry expands from tetra- to hexacoordination on interaction with solvent/H_2O_2 molecules.

Interconversions between Hydroperoxide and Superoxide

The intensity of EPR signals depends on the population difference (n) of the two spin quantized energy levels ($M_s = \pm 1/2$). According to the Boltzmann function, the population difference is given by the expression (35)

$$n = N \tanh(\Delta E/2kT), \qquad [2]$$

where N is the total number of spins, k is Boltzmann's constant, T is absolute, temperature, and ΔE is the energy separation between the two spin quantized energy levels. If $\Delta E/2kT < 1$, which is the case in the present experiment, then the population difference can be rewritten as

$$n \approx (N/2)(\Delta E/kT). \qquad [3]$$

Hence, the intensity of the EPR signal varies linearly with $1/T$. The actual variation (Fig. 3) is, however, different from Eq. [3] for both TS-1 and TiMCM-41 samples. Two features may be noted in Fig. 3: (i) At low temperatures, the intensity of the EPR signals deviates from linearity and is less than that calculated from Eq. [3] (ii) The concentration of EPR-active superoxides varies as TiMCM-41 (CH_3OH; 9.521) > TS-1 (CH_3OH; 7.039) > TS-1 (CH_3CN; 2.763) (Fig. 3; curves c, b, and a, respectively). The lower EPR intensity can be explained if part of the EPR-active superoxides are converted into EPR-inactive oxo-titanium species such as hydroperoxides/peroxides at lower temperatures. Our results (Fig. 3 and Table 1) indicate that the formation of the hydroperoxide/peroxides depends on both the titanosilicate (hydroperoxides/peroxides are formed more readily on TS-1 than on TiMCM-41) and solvent (more hydroperoxides/peroxides in the presence of CH_3CN). The relative EPR signal intensity (Table 1) of superoxide species is smaller in TS-1 than in TiMCM-41 as a larger amount of oxo-titanium species is in the form of EPR-inactive hydroperoxide/peroxide in TS-1 while it is in the form of the EPR-active superoxides in TiMCM-41.

The *in situ* EPR studies reveal that species A and C of TS-1 are consumed after the catalytic reaction (the intensities of signals due to A and C are reduced on addition of allylalcohol). This is, perhaps, due to their higher reactivity (compared to species B) in the oxidation of allylalcohol to the corresponding epoxide. Another possibility is that species A and C are transformed more easily to hydroperoxides or peroxides that actually perform the catalytic oxidation. The catalytic conversion of AA is also higher (95–96 wt%) in CH_3CN and $(CH_3)_2CO$ than in the more polar CH_3OH and C_2H_5OH (52–58 wt%) (23). The overall EPR signal intensity (Table 1) is lower in CH_3CN than in CH_3OH, indicating that active hydroperoxide species formation is more common in the former than in the latter solvent. The higher concentration of hydroperoxide/peroxide species in CH_3CN is perhaps responsible for the higher activity. In other words, a relationship between the type of oxo-titanium species and the catalytic activity/selectivity is suggested. The reversible expansion of the Ti coordination from 4 to 6 and the interconversion between Ti(IV)-superoxides and Ti(IV)-hydroperoxides/peroxides, characteristic of species A and C, may be crucial factors for the greater catalytic activity of titanosilicates containing species A and C. Such superoxide–hydroperoxide interconversions are, of course, well known in the chemistry of enzymes (36). Superoxide–peroxide interconversions are also known in MoO_x–Al_2O_3 (37) and CoO_x–MgO (38) systems. In some systems, especially TS-1–H_2O–H_2O_2, the EPR signal intensity (Table 1) is 1–2 orders of magnitude higher than in most other systems. This is important because the studied reaction mixture always contains water as a solvent of the H_2O_2. The observations suggest that when water alone is

present as solvent the preponderance of superoxide species is higher than when an organic solvent–water mixture is present. Species B mostly remained unchanged even at 77 K. TiMCM-41, generating mainly type B species on interaction with H_2O_2, is hence less active and selective than TS-1. In addition, TiMCM-41 generates less hydroperoxides/peroxides (from superoxides) than TS-1 (Fig. 3). This may be an additional factor contributing to the lower catalytic activity/selectivity of the former.

CONCLUSIONS

Interaction of TS-1 and TiMCM-41 with 30% aqueous H_2O_2 generates paramagnetic Ti(IV)-superoxide radical species, identified by EPR spectroscopy. Three different types of oxo-titanium species (A, B, and C, respectively) were identified in TS-1. All three superoxides, as well as the EPR-invisible hydroperoxides/peroxides, are associated with framework Ti(IV) ions. Mainly species B was identified over TiMCM-41. Variable-temperature EPR studies have revealed that species A and C undergo conversion to hydroperoxide/peroxide at low temperatures. The diamagnetic Ti(IV)–hydroperoxide/peroxide was formed in greater quantity at low temperatures and in solvents, such as CH_3CN. Species B mostly remained unchanged and did not convert to the hydroperoxide even at 77 K. The differences in the catalytic activity and selectivity of TS-1 and TiMCM-41 arise from, among other factors, the differences in the type and concentration of the oxo-titanium species that are generated during their interaction with H_2O_2.

REFERENCES

1. Notari, B., *Adv. Catal.* **41**, 253 (1996).
2. Vayssilov, G. N., *Catal. Rev.—Sci. Eng.* **39**, 209 (1997).
3. Lopez, A., Tuilier, M. H., Guth, J. L., Delmotte, L., and Popa, J. M., *J. Solid State Chem.* **102**, 480 (1993).
4. Bordiga, S., Coluccia, S., Lamberti, C., Marchese, L., Zecchina, A., Boscherini, F., Buffa, F., Genoni, F., Leofanti, G., Petrini, G., and Vlaic, G., *J. Phys. Chem.* **98**, 4125 (1994).
5. Taramasso, M., Perego, G., and Notari, G., U.S. Patent. 4,410,501 (1983).
6. Perego, G., Bellussi, G., Corno, C., Taramasso, M., Buonomo, F., and Esposito, A., *Stud. Surf. Sci. Catal.* **28**, 129 (1986).
7. Millini, R., Previde Massara, E., Perego, G., and Bellussi, G., *J. Catal.* **137**, 497 (1992).
8. Huybrechts, D. R. C., Buskens, P. L., and Jacobs, P. A., *J. Mol. Catal.* **71**, 129 (1985).
9. Bellussi, G., Carati, A., Clerici, M. G., and Esposito, A., *Stud. Surf. Sci. Catal.* **63**, 421 (1991).
10. Clerici, M. G., and Ingallina, P., *J. Catal.* **140**, 71 (1993).
11. Thangaraj, A., Kumar, R., and Ratnasamy, P., *J. Catal.* **131**, 294 (1991).
12. Thangaraj, A., Sivasanker, S., and Ratnasamy, P., *J. Catal.* **131**, 394 (1991).
13. Tuel, A., Diab, J., Gelin, P., Dufaux, M., Dutel, J.-F., and Ben Taarit, Y., *J. Mol. Catal.* **63**, 95 (1990).
14. Prakash, A. M., and Kevan, L., *J. Catal.* **178**, 586 (1998).
15. Prakash, A. M., and Kevan, L., *Proceedings 12th International Zeolite Conference* 2625 (1999).
16. Bal, R., Chaudhari, K., Srinivas, D., Sivasanker, S., and Ratnasamy, P., *J. Mol. Catal. A: Chemical* **162**, 199 (2000).
17. Corma, A., Navarro, M. T., and Perez Pariente, J., *J. Chem. Soc. Chem. Commun.* 147 (1994).
18. Kresge, C. T., Leonowicz, M. E., Roth, W. J., Vartuli, J. C., and Beck, J. S., *Nature* **359**, 710 (1992).
19. Tanev, P. T., Chibwe, M., and Pinnavaia, T. J., *Nature* **368**, 321 (1994).
20. Beck, J. S., Vartuli, J. C., Roth, W. J., Leonowicz, M. E., Kresge, C. T., Schmitt, K. D., Chu, C.-T. W., Olson, D. H., Sheppard, E. W., McCullen, S. B., Higgins, J. B., and Schlenker, J. L., *J. Am. Chem. Soc.* **114**, 10834 (1992).
21. Biz, S., and Occelli, M. L., *Catal. Rev.—Sci. Eng.* **40**, 329 (1998).
22. Parton, R. F., Huybrechts, D. R. C., Buskens, Ph., and Jacobs, P. A., *Stud. Surf. Sci. Catal.* **65**, 47 (1991).
23. Bhaumik, A., Kumar, R., and Ratnasamy, P., *Stud. Surf. Sci. Catal.* **84**, 1883 (1994).
24. Thangaraj, A., Kumar, R., Mirajkar, S. P., and Ratnasamy, P., *J. Catal.* **130**, 1 (1991).
25. Thangaraj, A., Eapen, M. J., Sivasanker, S., and Ratnasamy, P., *Zeolites* **12**, 943 (1992).
26. Barrett, E. P., Joyner, L. G., and Halenda, P. P., *J. Am. Chem. Soc.* **73**, 373 (1951).
27. Geobaldo, F., Bordiga, S., Zecchina, Z., Giamello, E., Leofanti, G., and Petrini, G., *Catal. Lett.* **16**, 109 (1992).
28. Huybrechts, D. R. C., Vaesen, I., Li, H. X., and Jacobs, P. A., *Catal. Lett.* **8**, 237 (1991).
29. Che, M., and Tench, A. J., *Adv. Catal.* **32**, 1 (1983).
30. Che, M., and Giamello, E., *Stud, Surf. Sci. Catal.* **57 B**, 265 (1990).
31. Kanzig, W., and Cohen, M. H., *Phys. Rev. Lett.* **3**, 509 (1959).
32. Davydov, A. A., Komarova, M. P., Anerfrieneo, V. F., and Maksimov, N. G., *Kinet. Katal.* **14**, 1519 (1973).
33. Anpo, M., Che, M., Fubini, B., Garrone, E., Giamello, E., and Pagamini, M. C., *Top Catal.* **8**, 189 (1999).
34. Hijar, C. A., Jacubinas, R. M., Eckert, J., Henson, N. J., Hay, P. J., and Ott, K. C., *J. Phys. Chem. B* **104**, 12157 (2000).
35. Box, H. C., "Electron Paramagnetic Resonance Spectroscopy." Academic Press, New York (1997).
36. Siegbahn, P. E. M., and Crabtree, R. H., *Structure Bond.* **97**, 125 (2000).
37. Che, M., McAteer, J. C., and Tench, A. J., *Chem. Phys. Lett.* **31**, 145 (1975).
38. Giamello, E., Sojka, Z., Che, M., and Zecchina, A., *J. Phys. Chem.* **90**, 6084 (1986).